Original Research

Computationally Assessed 3D Anatomical Proximities and Spatial Relationships Among the Tricuspid Valve Annulus, Right Coronary Artery, and Triangle of Koch: Implications for Transcatheter Tricuspid Annuloplasty Repair

Jorge D. Zhingre Sanchez, PhD, Paul A. Iaizzo, PhD [*]

Departments of Surgery and Biomedical Engineering, Institute for Engineering in Medicine, University of Minnesota, Minneapolis, Minnesota, USA

ARTICLE INFO

ABSTRACT

Background: Transcatheter-based annuloplasty therapies for tricuspid regurgitation have demonstrated significant development over recent years. However, the tricuspid valve and neighboring vasculature and conductive tissue regions can present anatomical and device deployment challenges. This present study investigated the anatomical dimensions and spatial relationships of the cardiac structures essential to percutaneous annuloplasty procedures: the tricuspid annulus (TA), right coronary artery (RCA), and triangle of Koch border region.
Methods: Measurements were derived from computational three-dimensional reconstructions of static magnetic resonance imaging scans of perfusion-fixed human hearts (n = 82) with preserved right-sided heart anatomies. This specimen set included heart samples presenting with prediagnosed atrioventricular valvular regurgitation.
Results: Our anatomical assessments demonstrated that the TA to RCA proximities were intensified with the presence of atrioventricular valvular regurgitation, compared with healthy heart specimens. The minimal distances were frequently located between the lateral and posterior annular points. This annular region corresponds to the RCA distal segments and posterior descending branch origins. Greater portions and incidences of the RCA coursing parallel or inferior to the TA plane were recorded for these diseased hearts. Patient demographic variables (gender, age, and body mass index) were insignificant determinants of change for a majority of our results.
Conclusions: These three-dimensional reconstructions provide insights to guide the development and future iterations of transcatheter tricuspid valve annuloplasty systems with regards to device anchoring, annular geometry, tissue proximities, and implantation considerations.

ABBREVIATIONS

A, anterior; AL, anterolateral; APC, anteroposterior commissure; APCP, anteroposterior commissural point; AS, anteroseptal; ASC, anteroseptal commissure; ASCP, anteroseptal commissural point; AV, atrioventricular; CS, coronary sinus; L, lateral; MR, mitral regurgitation; MV, mitral valve; P, posterior; PL, posterolateral; PS, posteroseptal; PSC, posteroseptal commissure; PSCP, posteroseptal commissural point; RCA, right coronary artery; S, septal; TA, tricuspid annulus; TK, triangle of Koch; TR, tricuspid regurgitation; TV, tricuspid valve.

Introduction

Secondary or functional tricuspid regurgitation (TR) is categorized as the asymmetric right ventricular and tricuspid valve (TV) annular dilatation.[1-4] Percutaneous TV systems mimic surgical annuloplasty repair to correct for annular dilatation by implanting a prosthetic ring or suture device. Translating these surgical techniques to a transcatheter approach presents technical challenges due to complex TV anatomies.[2-5] Specifically, the coronary vasculature and cardiac conduction system surrounding the tricuspid annulus (TA) require careful assessment. Adjacent vasculature within proximity to the TA include the right coronary artery (RCA), which courses along the right atrioventricular (AV) groove, and the coronary sinus (CS) ostium. The septal region of the TA serves as a border that defines the triangle of Koch (TK), which is an anatomical landmark for the conductive AV nodal cells.[2-4,6]

---

* Address correspondence to: Paul A. Iaizzo, PhD, University of Minnesota, B172 Mayo, 420 Delaware St. SE, MMC 195, Minneapolis, MN 55455
    E-mail address: iaizz001@umn.edu (P.A. Iaizzo).

Suture and ring/band annuloplasty procedures have resulted in favorable patient outcomes with limited complications. However, the spatial proximities between the TA and neighboring cardiac structures present risks for iatrogenic damage. There have been exceptional cases where direct injury, distortion, or occlusion to the RCA has resulted from TV annuloplasty.[7,8] Although suture-induced RCA injuries are rare incidences, they are often underdiagnosed and may cause clinical complications, including right ventricular infraction, percutaneous intervention, bypass revascularization, and ring/suture removal.[7] Conduction disturbances and electrical instabilities may also result from TV annuloplasty and RCA injuries. Lesions or decreased blood flow to the RCA has been associated with acute myocardial infarctions and AV nodal branch blockage.[8,9] Population studies have reported relatively high rates of permanent pacemaker implantations following TV annuloplasty repairs, with the use of a ring or band emerging as a significant predictor for postoperative conduction disturbances.[10,11]

These complications remain a consideration for transcatheter tricuspid annuloplasty technologies. Multiple devices and systems are in development with a myriad of rings, anchors, and suturing designs being employed.[1-3,12] Preprocedural planning and intraprocedural imaging are essential for assessing the TA dimensions, anchoring sites, and proximities to the RCA.[2,4,5] However, these measurements are often limited to two-dimensional (2D) perspectives using cross-sectional planes in echocardiography and computed tomography. An enhanced assessment of these TV structures utilizing three-dimensional (3D) methodologies may provide further insights. Evaluating these anatomical structures that border the TA is important for interventional considerations to minimize the risk of coronary injuries and/or conductive tissue perforation.[1,4,5] To date, the minimal distances from the RCA to the TA for transcatheter therapies have yet to be analyzed.[13]

The present study primarily quantifies the anatomical dimensions, minimal distances, proximities, and spatial relationships between the TA and adjacent structures: the RCA, CS ostium, and TK septal border. These measurements were calculated using precise 3D computational reconstructions of TV anatomies from a large series of ex vivo human heart specimens, including those with TR. Our analyses provide anatomical specifications and design criteria as potential implications for transcatheter TV annuloplasty systems, such as annular geometry, anchoring/suturing depths, and implantation considerations.

Materials and Methods

Study Population, Disease States, and Heart Specimen Imaging

The ex vivo human hearts investigated in the present study (n = 82) were perfusion fixed and preserved to an approximate end-diastolic state.[14,15] The donor patient demographics and relevant cardiac histories were recorded (Supplemental Table 1). These heart specimens were divided into 3 disease state groups for comparison: Group I consisted of hearts without AV valvular disease but presenting with other structural diseases and/or no cardiac history (n = 52); group II was comprised of specimens with AV valvular regurgitation, including TR and/or mitral regurgitation (MR) (n = 30); and group III included hearts with AV valvular regurgitation as the primary disease state, excluding other structural diseases (n = 12). We performed static magnetic resonance imaging (MRI) of each heart specimen with a 3 Tesla Siemens Trio scanner (Siemens, Malvern, Pennsylvania). Each heart was scanned in the long-axis, both vertical and horizontal, and short-axis cardiac planes (Figure 1).

Three-Dimensional Modeling and Reconstructions

These high-resolution scans were imported into a Mimics medical image processing and modeling software program (Materialize NV; Leuven, Belgium) to generate detailed 3D anatomic models. The entire valvular tissue, right atrial/ventricular myocardium, and coronary
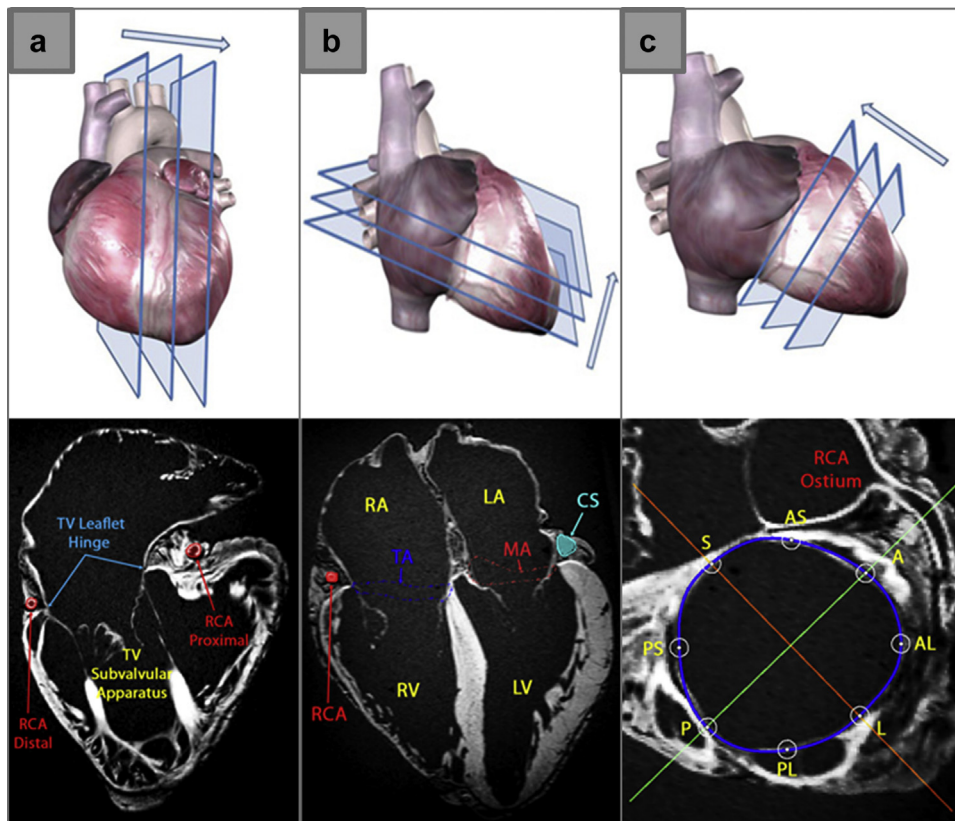
Figure 1. Static heart MRI stack sequence and scan data sets in 3 cardiac planes: (a) Vertical long-axis (2-chamber view); (b) horizontal long-axis (4-chamber view); (c) short-axis (atrioventricular base view). The corresponding scan data sets for all MRI stack sequences have an average of 484.2 (+72.3) pixel resolutions.
Abbreviations: A, anterior; AL, anterolateral; AS, anteroseptal; CS, coronary sinus; L, lateral; LA, left atrium; LV, left ventricle; MA, mitral annulus; P, posterior; PL, posterolateral; PS, posteroseptal; RA, right atrium; RCA, right coronary artery; RV, right ventricle; S, septal; TA, tricuspid annulus; TV, tricuspid valve.

vasculatures were segmented and reconstructed. Each right heart 3D model was sliced to provide atrial and ventricular views of the TV apparatus, RCA, CS ostium, and AV junction (Figure 2).

Anatomical Landmarks and Analysis

The multiplanar MRI scans and reconstruction models were used to mark specific anatomical points along each TV and RCA vessel (Figure 3). The TA spline was marked using the leaflet hinge points and segmented into 8 annular points based on topographic or surgical classification: septal (S), anteroseptal (AS), anterior (A), anterolateral (AL), lateral (L), posterolateral (PL), posterior (P), and posteroseptal (PS).[6,16,17] The TV commissures were defined as the leaflet indentation regions, divided by the fan-shaped chordae from the 3 major papillary muscles, and marked as the anteroseptal (ASCP), anteroposterior (APCP), and posteroseptal (PSCP) commissural points.[18,19]

The RCA vessel was modeled, from the ostium to the posterior right ventricle, to identify the origins of the branching acute marginal and posterior descending arteries. These branching vessel points were used to divide the RCA centerline into the proximal, mid, and distal segments.[20] The majority of heart specimens in this study (91.5%) presented with right-dominant circulation, with the posterior descending artery originating from the RCA. For left-dominant hearts, the vessel terminal end was marked at the crux cordis on the posterior ventricular surface.

For this study, the TK border along the septal leaflet hinge line, or anterior edge, was the region of interest. The TK anterior edge was defined as the segment from the central fibrous body center, or apex, and the tangential intersection between the CS ostium and septal leaflet annulus.[6,21] For each TV reconstruction, the ASCP was estimated as the TK apex.

Data Acquisition and Statistical Analyses

The structure data points were analyzed using MATLAB (Natick, Massachusetts) and Minitab Statistical Software (State College, Pennsylvania). The resulting measurements were analyzed for the entire study population and then compared between heart groups (I-III) based on disease states. Anatomical dimensions and spatial parameters were presented as mean ($\pm$ standard deviation) and frequencies, respectively. Changes between heart groups were expressed as percent differences. We performed statistical analyses for continuous and categorical variables using the Student's t-test, or analysis of variance, and chi-square (χ2) test, respectively. A *p-value* less than 0.05 was considered statistically significant.

Results

Anatomical Parameters

The dimensions and parameters of the TA and RCA segments were measured for each computational heart reconstruction (Table 1, Supplemental Table 2). The average total TA perimeter for the entire study population was 129.7 mm ($\pm$13.1). An increasing trend of leaflet annuli base, or circumferential length from posterior to anterior to septal, was measured for all disease groups. Each TA orifice area and best-fit diameters were calculated from the 3D annuli spline projected on the TV plane. The TK border averaged a length of 32.0 mm ($\pm$7.3), which equated to approximately 66.5% ($\pm$15.1) of the septal leaflet base length. The average total RCA vessel length, from the ostium to the posterior descending branch, was 115.3 mm ($\pm$16.6) for the whole sample size. The average proximal-mid and distal segment lengths decreased within AV valvular regurgitant hearts.

Proximities and Minimal Distances

The 3D spatial distances between each TA and circulating RCA vessel were calculated. For the control sample size, the average minimal distance between these structures was 6.8 mm ($\pm$2.2). Most noticeably, the hearts with AV valvular regurgitation (groups II and III) exhibited distances approximate to or less than 6 mm (Figure 4a). The proximities between the TA and CS ostia were also recorded (Supplemental Table 3). The minimal distances between the RCA segments and branches to the
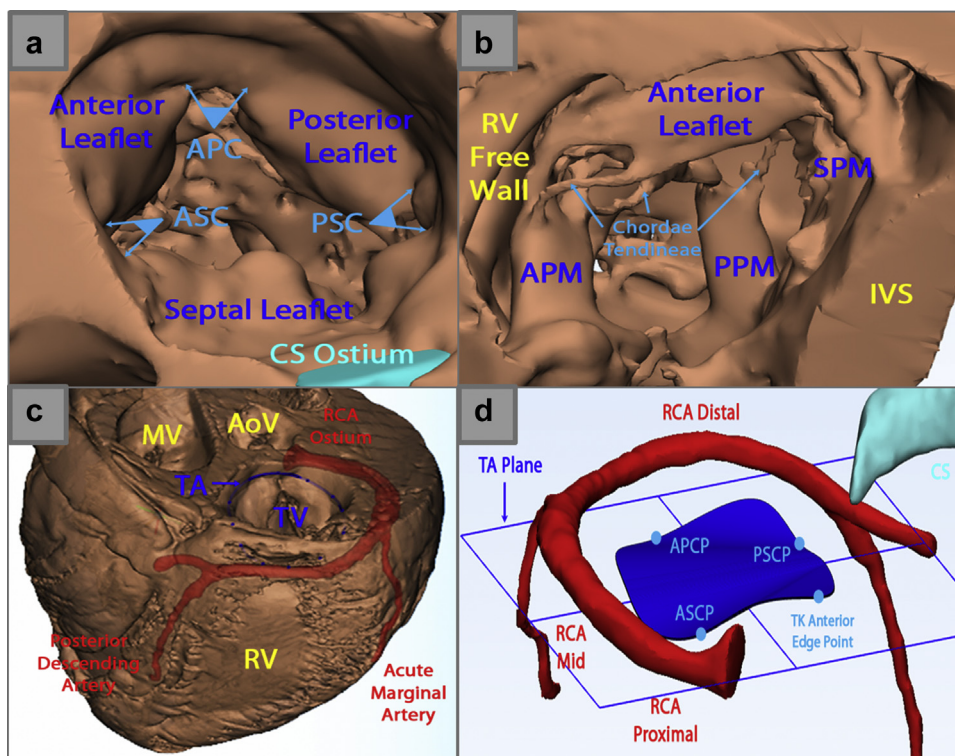
Figure 2. Three-dimensional volume reconstructions of right heart anatomies. (a) Right atrial view of tricuspid valve, commissures, and triangle of Koch region. (b) Inferior view of subvalvular apparatus with papillary complexes and chordae tendineae. (c) Whole tissue model of ventricular base and right coronary artery vasculature with branching arteries. (d) Isolated reconstructions of tricuspid annulus with commissural points, right coronary artery segments, and coronary sinus vessel.
Abbreviations: AoV, aortic valve; APC, anteroposterior commissure; APCP, anteroposterior commissural point; APM, anterior papillary muscle; ASC, anteroseptal commissure; ASCP, anteroseptal commissure point; CS, coronary sinus; IVS, interventricular septum; MV, mitral valve; PPM, posterior papillary muscle; PSCP, posteroseptal commissural point; RCA, right coronary artery; RV, right ventricle; SPM, septal papillary muscle; TA, tricuspid annulus; TK, triangle of Koch; TV, tricuspid valve.
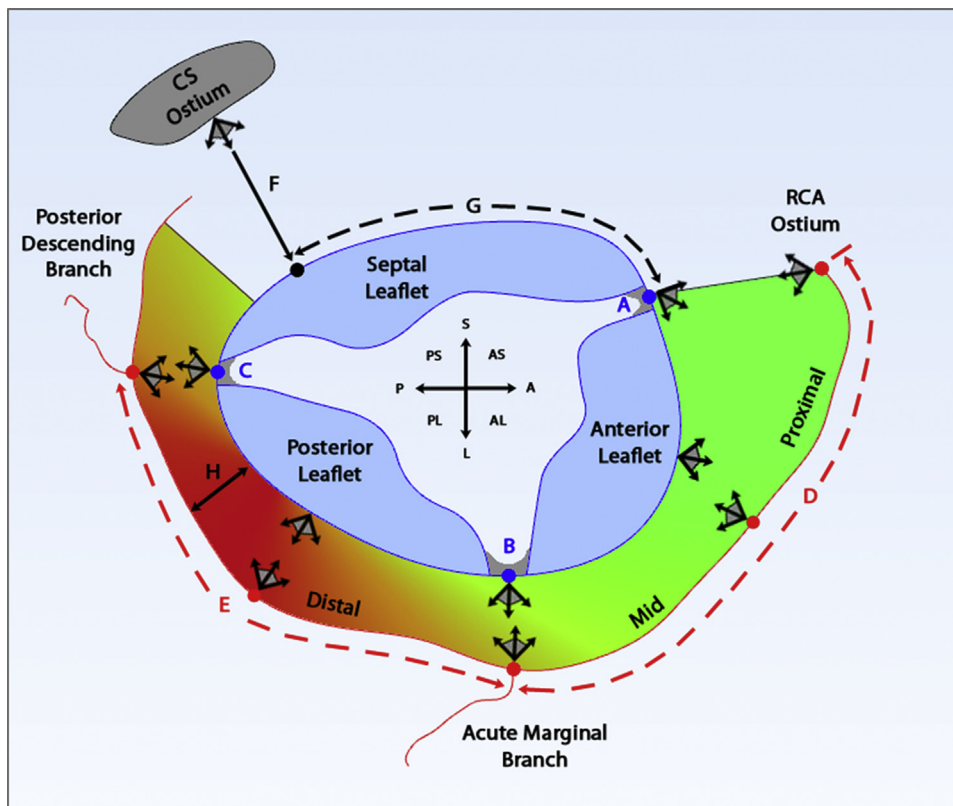
Figure 3. Schematic diagram of splines and coordinate points marked for 3D computational measurement analyses. The proximities and lengths were measured along the entire tricuspid annulus and right coronary artery (shaded region). The minimal distances between tricuspid valve commissures, annular points, right coronary artery segments, and coronary sinus ostium were calculated. (a) Anteroseptal commissural point to the right coronary artery. (b) Anteroposterior commissural point to the right coronary artery. (c) Posteroseptal commissural point to the right coronary artery. (d) Right coronary artery proximal-mid segment length. (e) Right coronary artery distal segment length. (f) Coronary sinus ostium to tricuspid annulus. (g) Triangle of Koch border annuli length. (h) Absolute minimal distance between the entire tricuspid annulus and right coronary artery.

Abbreviations: A, anterior; AL, anterolateral; AS, anteroseptal; CS, coronary sinus; L, lateral; P, posterior; PL, posterolateral; PS, posteroseptal; RCA, right coronary artery; S, septal.

TA plane were compared between disease groups (Figure 4b). Hearts with AV valvular regurgitation exhibited the closest proximities along the plane level, with the proximal-mid segment consistently having the minimum value (0.5 ± 2.9 mm for group II; 1.6 ± 2.3 mm for group III).

Spatial Assessment

The spatial relationships and minimal distances between each TV annular point and the nearest RCA segment were compared for heart specimens with (group II) or without (group I) AV valvular regurgitation (Figure 5a and b). The posterior leaflet, specifically the TA regions between the PL and P points, was most frequently the site of closest proximity to the RCA for the whole study population (72.0%) and both disease states (53.9% for group I; 40.0% for group II). The prevalence of each RCA segment and branch coursing below the TA plane was recorded (Figure 5d). The proximal-mid segments most frequently curved beneath the TA (23.1%) for hearts without AV valvular regurgitation and demonstrated a significant increase within group II (46.7%). Furthermore, the presence of AV valvular regurgitation correlated with significant increases in spatial proximities between the RCA and TA (Figure 5c).

Computational 3D Model Reconstructions

Computational 3D reconstructions of the healthy or nondiseased control specimens were compared with hearts with only AV valvular regurgitation (group III), to derive the percentage difference in the proximities and spatial measurements. The TA annulus shape and tissue depths were derived based on the 3D positions of the annular points to the TA plane, or AV groove, and RCA, respectively (Figure 6a and b). The presence of AV valvular regurgitation resulted in decreased average tissue depths, or greater proximities, between all TA points and RCA segments. Furthermore, the minimal distance points along the entire TAs to the nearest RCA segments in group III specimens decreased by 23.6% compared with the control (Figure 6d).

The RCA coursing positions and overlap angles at the minimal distance points relative to the AV planes were analyzed (Figure 6c and d). A positive or negative overlap angle indicated that the RCA coursed superior ($34.3° \pm 17.7°$) or inferior ($-15.0° \pm 14.7°$) to the TA, respectively. Compared with the control group, the hearts with only AV valvular regurgitation displayed an RCA shift toward the plane, most noticeably with a percentage decrease for distal points (70%) and a greater coursing angle ($36.0° \pm 15.1°$).

Discussion

Implications for Transcatheter Tricuspid Annuloplasty Systems

Ring Anchoring Depths and Annular Geometry

Appropriate anchoring and implant designs based on TV anatomies are critical parameters for performing transcatheter ring annuloplasty procedures. Current annuloplasty systems secure a fabric sleeve or nitinol ring to the annulus using stainless steel screws, anchors, or stakes that are commonly 6 mm in length. The material and number of anchors vary depending on the system implant size for annular fixation.[1-3,12]

The device specifications for these transcatheter rings were primarily designed for the mitral valve (MV) and tested for treating MR. Previous anatomical studies that analyzed the proximities between the MV and adjacent left-sided vasculature, including patients with severe MR, reported average distances from the annulus to the CS ranging between 8.5 and 9.7 mm.[22-24] Spencer et al.[25] reported that the closest mean distances from the MV to the CS and left circumflex artery were 9.0 and 7.8 mm at the posterior commissural positions, respectively. However, our study reports the minimal distances and proximities of the TA to surrounding vasculatures to be consistently lower.

For our entire study population, the average minimal distance between the TA and the nearest RCA region was only 6.5 mm. These mean distances decreased considerably, between 5.3 and 6.0 mm, in the heart samples with AV valvular regurgitation. These average proximities from the TA to the RCA vessel are noticeably approximate or below the

Table 1

Anatomical parameters of tricuspid annulus and right coronary artery based on diseases states

Parameter	Study population	Control	AV valvular regurgitation		
	Total hearts (n = 82)	No relevant cardiac history (n = 22)	Group I (n = 52)	Group II (n = 30)	Group III (n = 12)
TV annuli					
TA perimeter (mm)	129.7 (13.0)	130.0 (14.4)	130.2 (13.1)	128.8 (13.2)	127.9 (13.6)
Leaflet base length (mm)					
Anterior	42.8 (7.3)	41.2 (7.2)	41.7 (7.4)	44.7 (6.8)	45.7 (5.8)
Posterior	37.6 (7.6)	39.5 (6.8)	38.2 (6.8)	36.5 (8.8)	34.2 (7.1)
Septal	49.2 (11.0)	49.3 (13.6)	50.2 (12.0)	47.5 (8.9)	47.9 (7.8)
TK border	32.0 (7.3)	31.2 (5.6)	32.2 (6.3)	31.7 (8.9)	33.4 (8.1)
TV orifice area (mm^2)	1252.4 (259.6)	1262.3 (297.8)	1265.7 (261.9)	1229.5 (258.5)	1217.6 (254.1)
Maximal diameter (mm)	44.5 (4.6)	44.6 (5.1)	44.6 (4.7)	44.4 (4.5)	44.4 (4.7)
Minimal diameter (mm)	36.6 (5.1)	37.0 (5.2)	37.1 (4.7)	35.8 (5.7)	35.6 (5.1)
RCA vessel					
RCA vessel length (mm)	115.3 (16.6)	115.7 (17.9)	117.0 (16.6)	112.2 (16.3)	107.0 (15.7)
Segment length (mm)					
Proximal-mid	51.3 (11.4)	49.7 (11.3)	51.3 (11.5)	51.4 (11.5)	47.7 (9.4)
Distal	64.0 (15.1)	65.9 (18.5)	65.8 (15.8)	60.8 (13.3)	59.3 (15.2)
Vessel diameter (mm)	3.6 (0.9)	3.4 (0.9)	3.6 (0.9)	3.6 (0.9)	3.4 (1.0)
Tortuosity	0.51 (0.07)	0.51 (0.07)	0.52 (0.06)	0.49 (0.01)	0.45 (0.08)

Notes. Differences between control and disease groups were not statistically significant. (*p* Values for these parameters are included in Supplemental Table 2).
AV, atrioventricular; RCA, right coronary artery; TA, tricuspid annulus; TK, triangle of Koch; TV, tricuspid valve.

previously reported anchor depth length (Figures 4a and 5a). Furthermore, the frequency of annular tissue depth within 6 mm gradually increased clockwise around the TA, from the A (1.2%) to P (22.0%) regions (Figure 6b). Our study results suggest that translating current anchoring systems for the TV should require further anchor refinement and technical details to account for these TA minimal distances and tissue depth range. The reported anchor lengths would be effective in the anterior regions but may need reconsideration at the posterior annulus.

The geometrical design of TV rings is important for avoiding postoperative conduction disorders. Surgical annuloplasty with complete sutured rings is effective for TR treatment but susceptible to conductive tissue damage. TV partial or incomplete rings, which stabilize the anterior and posterior regions, avoid suturing the septal annulus and reduce the incidence of conduction disturbances.[10,26] Although these partial rings demonstrate valid surgical outcomes in TR treatment, recurrent dilations of the PS annular area remain a concern. It has been noted that anchoring the rings beyond the posteroseptal commissure (PSC), while avoiding the septal conductive regions, may address this issue.[26] Transcatheter design modifications currently being implemented include the removal of the anchors near the AV node, optimal implant positioning, and partial ring openings.[2]

The TK border defined in our study represents the TA portions that should be avoided during annuloplasty. The septal leaflet region past the PSC suitable for suturing or ring implantation was 14.6 mm (±5.1) in length. The total perimeters or annular base lengths from the anteroposterior commissure (APC) to the TK anterior edge point averaged 94.5 mm (±10.5), which was a 4% decrease from healthy heart specimens. Based on these computational measurements, the partial ring contour lengths (∩) can safely be designed to approximately 74.0% (±5.1) of the TA (Figure 6a).

The 3D annular shapes and ring design specifications can be approximated using this study data. Our results agree with previous reports that analyzed the TV motion as a criterion for flexible and physiological annular ring design.[16,17,27] The highest points of the TA directed toward the right atria were the AS and P regions. The lowest points protruding toward the right ventricular apexes were the PS and S points (Figure 6a). Consistent with TR pathologies, the hearts with AV valvular regurgitation demonstrated a flattening of the annuli from saddle-shaped to planar configurations.[17] Additional TA dimensions to consider for ring design specifications, including orifice area and diameters, are listed in Table 1.

TV Commissure Proximities and Annular Suturing

Commissures and annular points are key anatomical markers for transcatheter direct suture-based annuloplasty systems that cinch and remodel the annulus. These suture-based technologies are currently designed to plicate the posterior leaflet by cinching pledgeted sutures or tensioned anchors near the APC, mid-anterior, or PS annular regions. Additional devices for achieving TV bicuspidization utilize multiple anchor designs, dacron bands, or nitinol stents deployed within the inferior vena cava.[1-3,12]

Knowledge of these commissural point proximities to the RCA may be useful for these techniques. In the present study, the average APCP and PSCP minimal distances to the RCA were 10.7 (±3.7) and 8.7 mm (±3.1), respectively. These distances decreased significantly in heart samples presenting with AV valvular regurgitation (Figure 6b). Furthermore, the minimal TA to RCA points were frequently neighboring the PSC (53.3%). With AV valvular regurgitation, these minimal points tend to shift toward the APC (58.8%) as the TA dilates (Figure 6d).

The A, AL, and PS annular points are common targets for TV suturing. Preclinical experiments of these systems noted that a tissue depth less than 4 mm between the anterior annular rim and RCA is insufficient.[28] The average minimal distances from the mid-anterior leaflet to the RCA gradually decreased from the A to AL points, 12.9 (±2.6) and 11.8 mm (±3.7), respectively. These distances significantly decreased in specimens with AV valvular regurgitation (Figure 5a). The PS locations for suturing are seemingly safe from RCA interaction with greater average distances of 17.5 mm (±5.6). Additionally, our results show that an insignificant percentage of the anterior (A to L) and posterior (PL to PS) leaflet regions were less than 4 mm in annular proximity to the RCA.

The annular base lengths of each leaflet also dictate the number of sutures, or suture width, that can be employed for these systems. Early clinical experience for these suture-based systems indicated that 5 anchors should be implanted between the APC and PSC at 10 mm length apart.[29] However, our results suggest that 3-4 sutures could be implanted along the posterior annulus using this suture width. Suturing 5 anchors would require smaller separations, ranging between 6.5 and 9.3 mm, to be feasible. AV valvular regurgitation further decreases these suture widths by 14.3% compared with healthy heart specimens (Figure 6d).

RCA Coursing Trajectory and Implantation

The spatial relationships between the RCA and TA, specifically the coursing path and inferior segments, should be considered for transcatheter ring and suture-based annuloplasty procedures. This also applies to indirect annuloplasty wire systems that circumferentially course along the AV groove, crossing the path of the coronary vessels, to tighten and compress the TA.[1-3,12] Vessel compressions are potential device complications that may require coronary protection. Portions of the RCA that
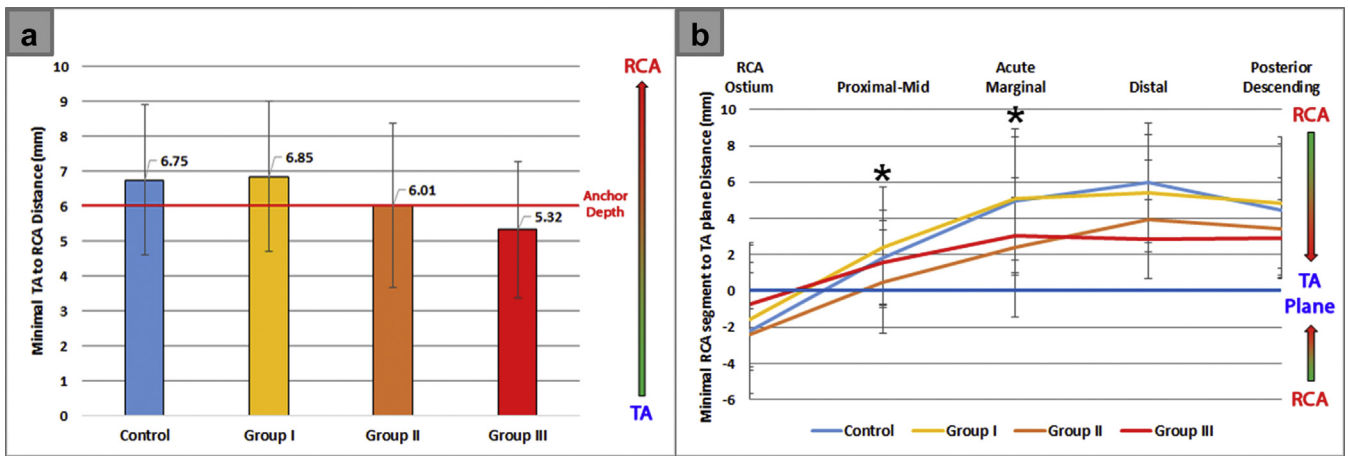
Figure 4. **Comparison of tricuspid annulus (TA) and right coronary artery (RCA) proximities between control and disease groups.** (a) Minimal distance from TA spline to RCA centerline, in relation to the common length (6 mm) of transcatheter annuloplasty anchors (red horizontal line). (b) Minimal distances from RCA segment midpoints and branching origins to the tricuspid annulus plane (blue horizontal line). The shaded arrows illustrate proximity gradient from maximum (green) to minimum (red) distances. *Statistical difference between heart groups.

course across this implant region may be susceptible to impingement or compression during annuloplasty. This risk is intensified with transcatheter procedures that deploy anchors and screws adjacent to the annular hinge and into the underlying basal RV tissue. The annular tissue depth, spatial location of the RCA, trajectory of the anchors, and angle of implantation are typically assessed during intraprocedural imaging.[5,30]

The coursing or overlap angles between the TA and RCA, at the minimal proximity points, averaged 33.3° (±18.0) (Figure 6d). Although a superior coursing trajectory was most prevalent (95.1%), approximately 35.4% of these heart specimens had a coursing angle less than 25°, including those that displayed a negative overlap angle due to an inferior RCA segment. These results suggest that the TA minimal distance points are often near parallel or in plane with the RCA. The frequency of

the RCA coursing across the AV groove and inferiorly to the TV annular plane was relatively high, as per our findings. The beginning portions of the RCAs were most frequently inferior (57.3%) along the ostium, proximal-mid segment, and acute margin branch origin. The probability of these occurrences was considerably higher than that in the inferior RCA distal segment portions (6.1%). Only 18.3% of the hearts presented with an RCA vessel that was entirely superior to the TA plane level. Furthermore, every RCA segment, except the ostium, shifted inferiorly toward the TA plane or AV groove in hearts diagnosed with AV valvular regurgitation (Figures 4b and 6c).

These results reveal a frequent observation of the RCA proximal and mid segments coursing within the trajectory path for these anchors, surgical sutures, or wires that commonly target the anterior annular
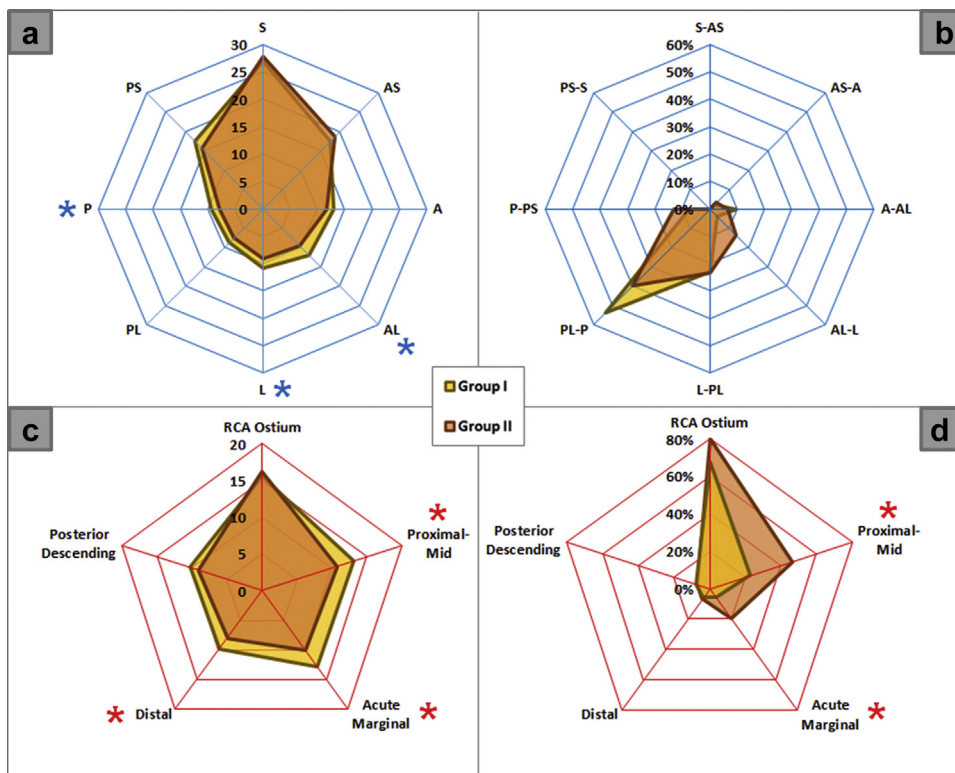
Figure 5. Radar graphs demonstrating spatial distributions of tricuspid annulus (TA)-right coronary artery (RCA) minimal distances, proximities, and inferior RCA segments for group I and II hearts. (a) TA points spatial proximities to RCA. (b) Spatial distribution of TA-RCA minimal distances. (c) RCA segment/branch spatial proximities to TA. (d) Spatial distribution of RCA segments/branches coursing inferior to TA plane. *Statistical difference between heart groups.
Abbreviations: A, anterior; AL, anterolateral; AS, anteroseptal; L, lateral; P, posterior; PL, posterolateral; PS, posteroseptal; S, septal.
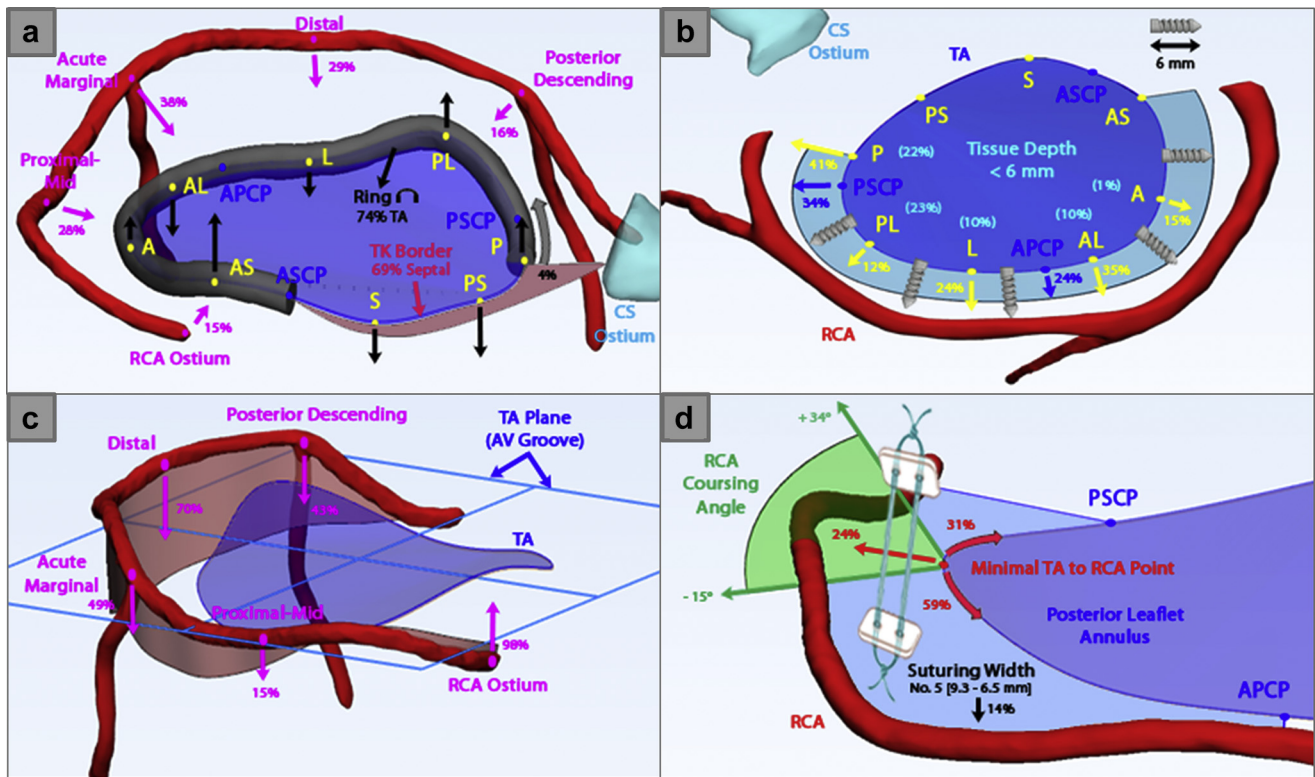
Figure 6. Computational 3D reconstructions and percentage differences of tricuspid annulus (TA)-right coronary artery (RCA) proximities, anatomical parameters, and spatial measurements between nondiseased (control) and atrioventricular valvular (AV) regurgitation (group III) heart specimens. Directional arrows represent percentage differences for these measurements. (a) TA points and triangle of Koch (TK) border region (red shading) define the TA shape for annuloplasty rings (grey band; ∩ = contour length). (b) Proximities and tissue depth between TA points to the RCA in relation to an anchor length of 6 mm (cyan shading). (c) Positioning change of RCA segments and branches (red shading) to the TA plane (AV groove). (d) Range of RCA coursing angles (green shading) to the TA plane at the closest proximity point and tissue depth along the posterior leaflet (blue shading) for suturing.

Abbreviations: A, anterior; AL, anterolateral; APCP, anteroposterior commissural point; AS, anteroseptal; ASCP, anteroseptal commissural point; CS, coronary sinus; L, lateral; P, posterior; PL, posterolateral; PS, posteroseptal; PSCP, posteroseptal commissural point; S, septal.

regions. Thus, careful consideration for device implantations should be taken to avoid RCA impingements or compressions.

Associated Literature

Previous cadaveric studies have established anatomic measurements between the TA and RCA. The results of these tissue studies were derived from 2D planar measurements using TV dissections and smaller heart sample sizes.[31,32] Other recent reports that utilized comprehensive CT imaging to assess the TV, using larger cohorts of patients with varying degrees of TR, provide comprehensive spatial measurements. To note, these CT studies used short- and long-axis chamber views to measure the 2D horizontal and vertical distances of the RCA to leaflet insertion levels or the AV groove.[13,33,34] The current clinical consensus is shifting toward utilizing 3D analyses for both TV assessments and diagnostic imaging.

Our methodology builds upon these assessments since it is derived from enhanced static MRI scans of perfusion-fixed human heart specimens to create 3D computational reconstructions. These models mimic the multiaxis views obtained from 3D imaging modalities, with minimal artifact (Figure 1), to distinguish the leaflet hinge points that define the true annulus and project the entire TV apparatus and RCA. The true Euclidean distances were calculated as opposed to 2D imaging measurements. Compared with some of the previously mentioned reports, our study provides a relatively larger heart sample size (n = 82). The TV commissural points to the neighboring RCA were compatible to previously established values. However, we recorded minimal distances that were notably lower for the hearts identified with AV valvular regurgitation as the primary disease state. In addition to the commissural points

and anterior/posterior leaflet insertion points, our study reports the proximities of the entire TA and RCA using defined annular points and vessel segments. Furthermore, our study provides spatial assessment of the overlap angles and annular interaction with inferiorly coursing RCA segments. Overall, our study results were consistent with the general anatomical trends observed in previous reports. This includes the attenuating proximity gradients to the RCA from the ASC to PSC regions and transmural measurements.

Study Limitations

All measurements were computationally derived from static MRI data sets of end-diastolic right heart anatomies. Analyzing the proximities and spatial distributions between the TA and RCA at mid-late diastole or extreme TV diastolic openings of the cardiac cycle is of interest and is consistent with the aforementioned anatomical literature. This study would benefit from a greater sample size of heart specimens, especially those presenting with increasing TR severity. Considering that a major cause of secondary TR is left-sided mitral disease,[1,4] we categorized hearts with a history of TR and/or MR as the diseased groups with AV valvular regurgitation (Supplemental Table 1). The degrees of TR and MR recorded for our specimen population ranged from mild to moderate levels. Although the severity levels of regurgitation were limited, this study population serves as an adequate representation of TV annular dilation with the TA diameters consistently measuring greater than 44 mm (Table 1). Despite these limitations, our findings may have relevant implications for TR annuloplasty therapies. Validations of our 3D computational measurements could be achieved with dissections of the

same heart samples, but these studies are limited based on the ability to preserve these unique specimens. Furthermore, the anatomical variations and heterogeneity of TVs, which can exhibit multileaflet and multiscallop configurations,[18,19,35] should be considered in future studies.

Conclusion

The field of transcatheter annuloplasty approaches is rapidly evolving but presents anatomical challenges, specifically potential damage to the vasculature and conductive tissue regions surrounding the TV. A thorough understanding of the proximities and spatial relationships between these anatomic structures and their relative variabilities can provide critical insights for those developing and/or deploying these transcatheter systems. Our present study established a database of accurate measurements of relevant anatomical parameters, minimal distances, and spatial assessments for the TA, RCA, and TK regions, utilizing computational 3D MRI reconstructions of preserved ex vivo right heart anatomies. Heart specimens without structural heart disease, and those with TR and/or MR, were assessed. Our computational analyses build upon previous literature values and are focused on critical parameters for percutaneous TV annuloplasty. The results from this study aid to identify potential implications for transcatheter annuloplasty systems relating to device design, anatomy criteria, and implantation considerations.

ORCIDs

Paul A. Iaizzo [ID] https://orcid.org/0000-0002-7661-352X

Supplementary Material

Supplemental data for this article can be accessed on the publisher's website.

References

1 Mangieri A, Montalto C, Pagnesi M, et al. Mechanism and implications of the tricuspid regurgitation: from the pathophysiology to the current and future therapeutic options. *Circ Cardiovasc Interv.* 2017;10:1-12. https://doi.org/10.1161/CIRCINTERVENTIONS.117.005043

2 Asmarats L, Puri R, Latib A, Navia JL, Rodés-Cabau J. Transcatheter tricuspid valve interventions: landscape, challenges, and future directions. *J Am Coll Cardiol.* 2018; 71:2935-2956. https://doi.org/10.1016/j.jacc.2018.04.031

3 Kolte D, Elmariah S. Current state of transcatheter tricuspid valve repair. *Cardiovasc Diagn Ther.* 2020;10:89-97. https://doi.org/10.21037/cdt.2019.09.11

4 Dahou A, Levin D, Reisman M, Hahn RT. Anatomy and physiology of the tricuspid valve. *JACC Cardiovasc Imaging.* 2019;12:458-468. https://doi.org/10.1016/j.jcmg.2018.07.032

5 Hahn RT, Nabauer M, Zuber M, et al. Intraprocedural imaging of transcatheter tricuspid valve interventions. *JACC Cardiovasc Imaging.* 2019;12:532-553. https://doi.org/10.1016/j.jcmg.2018.07.034

6 Faletra F, Leo LA, Paiocchi VL, et al. Imaging-based tricuspid valve anatomy by computed tomography, magnetic resonance imaging, two and three-dimensional echocardiography: correlation with anatomic specimen. *Eur Heart J Cardiovasc Imaging.* 2019;20:1-13. https://doi.org/10.1093/ehjci/jey136

7 Díez-Villanueva P, Gutiérrez-Ibanes E, Cuerpo-Caballero GP, et al. Direct injury to right coronary artery in patients undergoing tricuspid annuloplasty. *Ann Thorac Surg.* 2014;97:1300-1305. https://doi.org/10.1016/J.ATHORACSUR.2013.12.021

8 Morrissy SJ, Atkins BZ, Rogers JH. Iatrogenic right coronary artery stenosis resulting from surgical tricuspid valve replacement: case report and review of the literature. *Catheter Cardiovasc Interv.* 2014;84:1110-1114. https://doi.org/10.1002/ccd.25623

9 Cardoso R, Alfonso CE, Coffey JO. Reversibility of high-grade atrioventricular block with revascularization in coronary artery disease without infarction: a literature review. *Case Rep Cardiol.* 2016;2016:1971803. https://doi.org/10.1155/2016/1971803

10 Jokinen JJ, Turpeinen AK, Pitkänen O, Hippeläinen MJ, Hartikainen JEK. Pacemaker therapy after tricuspid valve operations: implications on mortality, morbidity, and quality of life. *Ann Thorac Surg.* 2009;87:1806-1814. https://doi.org/10.1016/j.athoracsur.2009.03.048

11 Jouan J, Mele A, Florens E, et al. Conduction disorders after tricuspid annuloplasty with mitral valve surgery: implications for earlier tricuspid intervention. *J Thorac Cardiovasc Surg.* 2016;151:99-103. https://doi.org/10.1016/j.jtcvs.2015.09.063

12 Curio J, Demir OM, Pagnesi M, et al. Update on the current landscape of transcatheter options for tricuspid regurgitation treatment. *Interv Cardiol.* 2019;14:54-61. https://doi.org/10.15420/icr.2019.5.1

13 van Rosendael PJ, Kamperidis V, Kong WKF, et al. Computed tomography for planning transcatheter tricuspid valve therapy. *Eur Heart J.* 2017;38:665-674. https://doi.org/10.1093/eurheartj/ehw499

14 Iaizzo PA. The Visible Heart® project and free-access website "Atlas of Human Cardiac Anatomy". *Europace.* 2016;18:163-172. https://doi.org/10.1093/europace/euw359

15 Anderson SE, Quill JL, Iaizzo PA. Venous valves within left ventricular coronary veins. *J Interv Card Electrophysiol.* 2008;23:95-99. https://doi.org/10.1007/s10840-008-9282-6

16 Knio ZO, Montealegre-Gallegos M, Yeh L, et al. Tricuspid annulus: a spatial and temporal analysis. *Ann Card Anaesth.* 2016;19:599-605. https://doi.org/10.4103/0971-9784.191569

17 Fukuda S, Saracino G, Matsumura Y, et al. Three-dimensional geometry of the tricuspid annulus in healthy subjects and in patients with functional tricuspid regurgitation. *Circulation.* 2006;114:492-498. https://doi.org/10.1161/CIRCULATIONAHA.105.000257

18 Sakon Y, Murakami T, Fujii H, et al. New insight into tricuspid valve anatomy from 100 hearts to reappraise annuloplasty methodology. *Gen Thorac Cardiovasc Surg.* 2019;67:758-764. https://doi.org/10.1007/s11748-019-01092-9

19 Kawada N, Naganuma H, Muramatsu K, Ishibashi-Ueda H, Bando K, Hashimoto K. Redefinition of tricuspid valve structures for successful ring annuloplasty. *J Thorac Cardiovasc Surg.* 2018;155:1511-1519. https://doi.org/10.1016/j.jtcvs.2017.12.045

20 Young PM, Gerber TC, Williamson EE, Julsrud PR, Herfkens RJ. Cardiac imaging: part 2, normal, variant, and anomalous configurations of the coronary vasculature. *Am J Roentgenol.* 2011;197:816-826. https://doi.org/10.2214/AJR.10.7249

21 Klimek-Piotrowska W, Hołda MK, Koziej M, Sałapa K, Piatek K, Hołda J. Geometry of Koch's triangle. *Europace.* 2017;19:452-457. https://doi.org/10.1093/europace/euw022

22 Nakamura K, Funabashi N, Naito S, et al. Anatomical relationship of coronary sinus/great cardiac vein and left circumflex coronary artery along mitral annulus in atrial fibrillation before radiofrequency catheter ablation using 320-slice CT. *Int J Cardiol.* 2013;168:5174-5181. https://doi.org/10.1016/j.ijcard.2013.07.261

23 Maselli D, Guarracino F, Chiaramonti F, Mangia F, Borelli G, Minzioni G. Percutaneous mitral annuloplasty: an anatomic study of human coronary sinus and its relation with mitral valve annulus and coronary arteries. *Circulation.* 2006;114:377-380. https://doi.org/10.1161/CIRCULATIONAHA.105.609883

24 Tops LF, Van de Veire NR, Schuijf JD, et al. Noninvasive evaluation of coronary sinus anatomy and its relation to the mitral valve annulus: implications for percutaneous mitral annuloplasty. *Circulation.* 2007;115:1426-1432. https://doi.org/10.1161/CIRCULATIONAHA.106.677880

25 Spencer JH, Prahl G, Iaizzo PA. The prevalence of coronary sinus and left circumflex artery overlap in relation to the mitral valve. *J Interv Cardiol.* 2014;27:308-316. https://doi.org/10.1111/joic.12106

26 Chikwe J, Anyanwu AC. Surgical strategies for functional tricuspid regurgitation. *Semin Thorac Cardiovasc Surg.* 2010;22:90-96. https://doi.org/10.1053/j.semtcvs.2010.05.002

27 Fawzy H, Fukamachi K, Mazer CD, et al. Complete mapping of the tricuspid valve apparatus using three-dimensional sonomicrometry. *J Thorac Cardiovasc Surg.* 2011; 141:1037-1043. https://doi.org/10.1016/j.jtcvs.2010.05.039

28 Khan JM, Rogers T, Schenke WH, et al. Transcatheter pledget-assisted suture tricuspid annuloplasty (PASTA) to create a double-orifice valve. *Catheter Cardiovasc Interv*. 2019;92:1-17. https://doi.org/10.1002/ccd.27531

29 Williams M. Minimally invasive tricuspid valve annuloplasty repair technology (MIATM, MicroInterventional Devices): early clinical experience. Presented at Transcatheter Cardiovascular Therapeutics Conference; September 21, 2018; San Diego, CA.

30 Prihadi EA, Delgado V, Hahn RT, Leipsic J, Min JK, Bax JJ. Imaging needs in novel transcatheter tricuspid valve interventions. *JACC Cardiovasc Imaging*. 2018;11:736-754. https://doi.org/10.1016/j.jcmg.2017.10.029

31 Lee Y-T, Chang C-Y, Wei J. Anatomic consideration of stitch depth in tricuspid valve annuloplasty. *Acta Cardiol Sin*. 2015;31:232-234. https://doi.org/10.6515/ACS20140929C

32 Ueda A, McCarthy KP, Sánchez-Quintana D, Ho SY. Right atrial appendage and vestibule: further anatomical insights with implications for invasive electrophysiology. *Europace*. 2013;15:728-734. https://doi.org/10.1093/europace/eus382

33 Saremi F, Pourzand L, Krishnan S, et al. Right atrial cavotricuspid isthmus: anatomic characterization with multi-detector row CT. *Radiology*. 2008;247:658-668. https://doi.org/10.1148/radiol.2473070819

34 Al Aloul B, Sigurdsson G, Can I, Li J, Dykoski R, Tholakanahalli VN. Proximity of right coronary artery to cavotricuspid isthmus as determined by computed tomography. *Pacing Clin Electrophysiol*. 2010;33:1319-1323. https://doi.org/10.1111/j.1540-8159.2010.02844.x

35 Hołda MK, Zhingre Sanchez JD, Bateman MG, Iaizzo PA. Right atrioventricular valve leaflet morphology redefined: implications for transcatheter repair procedures. *JACC Cardiovasc Interv*. 2019;12:169-178. https://doi.org/10.1016/j.jcin.2018.09.029